ASEAN Journal of Chemical Engineering 2024, Vol. 24, No. 3, 328 – 341

The Oxidation of Nanocellulose from Oil Palm Empty Fruit Bunch (OPEFB) by TEMPO/NaClO/NaBr

Annisa Amalia Ulfah
Muslikhin Hidayat *
Rochim Bakti Cahyono
Teguh Ariyanto
Chemical Engineering Department, Faculty of Engineering, Universitas Gadjah Mada, Jl. Grafika No.2, Kampus UGM, Yogyakarta, 55281
*e-mail: mhidayat@ugm.ac.id

Submitted 16 June 2024 *Revised* 26 November 2024 *Accepted* 2 December 2024

Abstract. One of the largest biomass wastes in Indonesia is oil palm empty fruit bunch (OPEFB), which produces thousands of tons of waste in a year. The value of biomass can be upgraded to nanocellulose-based adsorbents. Cellulose is extracted through three processes: delignification, bleaching, and hydrolysis. In this study, nanocellulose was oxidated with TEMPO (2,2,6-tetramethylpiperidine-1-oxyl radical)/NaClO/NaBr at pH 10 in a temperature room. The influence of oxidizer (NaClO 2, 4, 6, 8, and 10 mmol/gram) and catalysator (NaBr 25, 50, 100, 150, 200 mg/gram) in the formation of carboxylate groups and reaction time was studied. After the pretreatment process, cellulose content in the final product reached 61.8% with a crystallinity index of 58%. With lengths ranging from 127.4 nm to 512 nm and a diameter of less than 20 nm, nanocellulose is classified as cellulose nanofiber. Conductometry titration is used to find the carboxylate group formed on the nanocellulose surface. The highest carboxylate groups were found in 1,600 mmol/gram by adding 20 mmol/gram NaClO. As the addition of oxidants, degradation of nanocellulose occurred, which was indicated by a decrease in nanocellulose weight and shifting of function groups. All the reaction processes happened below 25 minutes, increasing the reaction rate by adding more than 50 mg/gram NaBr.

Keywords: Carboxylation, Cellulose Nanofiber, Oil Palm Empty Fruit Bunch, Oxidation, TEMPO

INTRODUCTION

Cellulose has been classified as a biomaterial discovered in various sources, including rice husks, algae, wood, and oil palm empty fruit bunches (OPEFB). It has emerged as the most commonly utilized component of lignocellulosic biomass (Hidayatulloh *et al.*, 2021). Indonesia ranks among the world's major palm oil producers, owning an abundance of oil palm empty fruit bunches (OPEFB) as solid waste.

Approximately 15,409,277 tons of OPEFB were produced from palm oil plantations (Badan Pengelola Dana Perkebunan Kelapa Sawit, 2023). This solid waste from oil production contains cellulose, hemicellulose, and lignocellulose, which can be optimized to create higher-value products. The percentage of cellulose from OPEFB is around 23.7–65.0% (Yiin *et al.*, 2019).

Nanocellulose can be isolated through a

DOI: 10.22146/ajche.14058

different process. The process itself affects the type of nanocellulose and categorizes it into three forms: crystalline nanocellulose (CNCs), cellulose nanofibers (CNF), and bacterial cellulose (BC). These three types of nanocellulose have similar chemical compositions but differ in other characteristics, such as morphological structure, particle size, crystallinity, and other properties. Nanocellulose properties depend on the biomass type (Zinge and Kandasubramanian, 2020). From these three types of nanocellulose, cellulose nanofiber is one of the most desired products in some research areas (Xu *et al.*, 2021). It has a small heat expansion coefficient, a favorable length-to-diameter ratio, and a large surface area. Cellulose nanofiber can be extracted from biomass through acid hydrolysis and delignification.

The hydroxide group in nanocellulose surfaces provides a negative charge and is bonded with wastewater ions and pharmaceutical waste during adsorption (Zinge and Kandasubramanian, 2020). In the advanced process of upgrading adsorbent capacities, the hydroxy group can be functionalized to other functional groups with higher bonding capabilities, such as carboxylate groups. Also, it can be transformed into a cation or anion, depending on the type of contaminants. From this sensible characteristic, nanocellulose is classified as a promising wastewater remediation adsorbent. The adsorption reaction contains various steps depending on the interaction between adsorbates and adsorbents. Some interactions occurred as physisorption, like van der Waals forces, chemisorption, and electrostatic adsorption through π-π bonding (Liu *et al.*, 2016).

Functionalization in nanocellulose surface depends on the process takes. Each process introduced different function groups and affected nanocellulose surface charge. It can be a negative or positive charge. The functionalization process is achieved by carboxymethylation, oxidation, phosphorylation, and sulfonation in the nanocellulose process. If the product needs high hydrophobicity, it can be processed through acetylation, amidation, and etherification (Bagheri and Julkapli, 2018; Thomas *et al.*, 2018). One of the simple methods to functionalize nanocellulose is chemical pretreatment. Pretreatment using sulfonate acid will introduce sulfonate group (SO_4^{2-}) and hydroxyl (-OH) groups (Singla *et al.*, 2019; Thomas *et al.*, 2018). Functionalization in nanocellulose is needed to aim for higher adsorbent capacity and produce hydrophobicity of nanocellulose surface to bond better with different solvents. Besides, functionalizing nanocellulose surfaces can enhance biocompatibility with contaminants and wastewater (Eyley and Thielemans, 2014).

Carboxylation is generally used to functionalize nanocellulose surfaces to attain carboxylate groups. One common substances the oxidation process is 2,2,6,6-tetramethylpiperidine-1-oxyl radical (TEMPO) (Isogai *et al.*, 2011). The oxidation process only takes on primary hydroxyl groups, while the secondary hydroxyl groups are unaffected (de Nooy *et al.*, 1994). It functionalizes C_6 alcoholic (-OH) groups in nanocellulose surfaces and converts them to carboxylic acid (-COOH) groups. Oxidation occurs when TEMPO forms nitroxyl radicals caused by a radical reaction with an oxidizer. The nitroxyl radicals will attack hydroxyl groups and turn into carboxylate groups through aldehydes as intermediates (Iwamoto *et al.*, 2011; Xhanari *et al.*, 2011).

Aldehyde groups formed during the oxidation reaction did not significantly alter the conditions, as it was rapidly converted (de Nooy *et al.*, 1995; Goldstein and Samuni, 2007). The formation of carboxylate groups during the process could influence the reaction conditions.

TEMPO oxidation occurs rapidly at room temperature, pH 10, and below aqueous conditions. Types of oxidizing agents and catalysts influence the reaction time and amount of carboxylate groups formed. Different combinations of oxidizers and catalysts have been studied. One of the common combinations is NaClO/NaBr/TEMPO. The NaClO (oxidizer) concentration variation will affect the carboxylated groups created in nanocellulose materials. The reaction time will affected by NaBr (catalyst) amount.

Several researchers have examined nanocellulose oxidation using bleached wood pulp (Thi Thanh Hop *et al.*, 2022), narrow-leaf cattail (Adawiyah *et al.*, 2022), hardwood (Levanič *et al.*, 2020), and oil palm empty fruit bunch (OPEFB) (Hastuti *et al.*, 2019). Research on cellulose oxidation from OPEFB has been conducted by varying the oxidizer NaClO (Hastuti *et al.*, 2019) and oxidizer $NaClO_2$ (Indarti *et al.*, 2015). In addition, experiments have also been conducted on the variation of time in the number of carboxylate groups formed (Martínez-Ramírez *et al.*, 2023). Nanocellulose from oxidized OPEFB has also been used for reinforcement in paper making and on alginate membranes for the water-ethanol separation process (Hastuti *et al.*, 2022). In the experiment on nanocellulose oxidation from OPEFB, no one has studied the addition of a catalyst (NaBr) to the rate of nanocellulose oxidation reaction, which will be explored in this study.

In this article, nanocellulose will be obtained from OPEFB through lignification and acid hydrolysis. The resulting nanocellulose will be characterized using TEM (Transmission Electron and Microscopy), PSA (Particle Size Analysis), and XRD (X-ray Diffraction). These characterization techniques will provide valuable insights into the structure, morphology, and properties of the nanocellulose. The study also investigated the influence of NaClO and NaBr combination in the formation of carboxylate groups and reaction time. The amount of carboxylate groups is found through conductometric titration.

MATERIALS AND METHODS

Materials

Oil palm empty fruit bunch (OPEFB) was purchased from PT. Teknologi Jaya Perkasa in Indonesia. Sodium hydroxide (NaOH) pellets 98%, hydrogen peroxide (H_2O_2) 30%, sulfuric acid (H_2SO_4) 98%, hydrochloric acid (HCl) 37%, sodium hypochlorite (NaClO) 5%, sodium bromide (NaBr) 99.99%, kalium bromide (KBr) all were purchased from Merck (Indonesia), and 2,2,6,6-tetramethyl-piperidine-1-oxyl (TEMPO) was purchased from Sigma Aldrich (USA).

Methods

Preliminary Process

Nanocellulose extraction

Pretreatment, which involved delignification and bleaching, was carried out before the acid hydrolysis process. The delignification process began by adding 10 g of OPEFB to a 17.5% NaOH solution and heating it at 90-95°C for 2 hours (Hidayatulloh *et al.*, 2022). This process separates lignocellulose from cellulose in the oil palm empty fruit bunch. The next step involved neutralizing the empty fruit bunch

with aquadest until it reached a pH of 7. Subsequently, the bleaching process was conducted by adding 10 gram delignified OPEFB using a 10% H_2O_2 solution for 2 hours at 80-90°C (Dewanti, 2018; Pranolo *et al.*, 2023) The neutralization process is required before the acid hydrolysis process to obtain nanocellulose. Acid hydrolysis was conducted by adding 10 gram bleached OPEFB using 40% H_2SO_4 for 1.5 hours at 50°C, with continuous stirring at 200 rpm (Husin, 2020; Soetaredjo *et al.*, 2022). Once the nanocellulose had been neutralized, it was then dried for 12 hours at 60°C.

Proximate analysis and Van Soest method

Proximate analysis and the Van Soest method were used to determine the lignin, hemicellulose, and cellulose. Two grams of OPEFB, D-OPEFB, B-OPEFB, and CNF were soaked in natural detergent fiber to remove other components besides lignin, hemicellulose, and cellulose. The substrate was then mixed with acid detergent fiber to remove hemicellulose and 72% sulfuric acid to remove cellulose. Lignin is the remaining component in this method. Water content was calculated by drying the substrate at 60°C. Ash content was estimated by taking the substrate to a furnace at 550°C.

Primary Process

Nanocellulose functionalization

One gram of nanocellulose was added to a 100 mL solution containing water, 32 mg/gram nanocellulose TEMPO, and NaBr (25-200 mg/gram nanocellulose). The suspension was mixed using a magnetic stirrer at 200 rpm. Sodium hypochlorite was subsequently added to the system in varying amounts of 4 - 20 mmol/gram nanocellulose to observe the effect of the oxidant on the final result of carboxylate groups (de Nooy *et al.*, 1994; Habibi *et al.*, 2006). The process was maintained at pH 10 by continuously monitoring the pH with a pH meter and adding 0.1 M NaOH as needed. The consumption of NaOH during the oxidation process was recorded. The reaction stopped 30 minutes after the pH did not change by adding 2 mL of methanol.

Reaction Result Analysis

Nanocellulose characterization

Transmission electron and microscopy

Transmission Electron and Microscopy (TEM) from JEOL JEM-1400 was used for the CNF characterization. TEM analysis helps to characterize nanocellulose in terms of exact morphology. The obtained CNF solution was diluted to 2 mg/mL before being injected into a copper grid. The electron beam was set at 120 kV.

Particle size analyzer

Particle Size Analyzer (PSA) from Microtrac Nanotrac Wave II was used to observe the nanocellulose size. The wet method was used as a particle size analyzer for cellulose. Cellulose nanofiber 0.03 gram was diluted in 10 mL water before being injected into PSA. The cellulose particle passed through a 6540-0.950 nm tube to calculate the particle size distribution.

X-ray diffraction

The crystallinity of nanocellulose was characterized using X-ray diffraction from Rigaku MiniFlex 600. X-ray diffraction operated at 40 kV and 40 mA radiation. X-ray diffractograms were scanned from 0 to 80 at a rate of 2 s/step with 0.02 step size. Crystallinity index (CrI) values were calculated from diffraction intensity data via the empirical method using Eq. (1) (Segal *et al.*, 1959).

$$CrI\ (\%) = \frac{I_{002} - I_{AM}}{I_{002}} \times 100\% \quad (1)$$

where I_{002} shows the maximum intensity of the reflection peak at $2\theta = 15^0$, and I_{AM} is the minimum value representing the amorphous reflection intensity at $2\theta = 45^0$.

Carboxylate analysis

The carboxyl groups in the nanocellulose surface were determined using a conductivity meter from LUTRON WAC-2019SD. Oxidized CNF 0.2 gram was diluted in 55 mL aquadest and 5 mL 0.01 M NaCl. Hydrochloride acid (HCl) 0.1 M was added to the solution until pH 3. Natrium hydroxide (NaOH) 0.01 M was added dropwise 0.1 mL/minute until pH 10.

FT-IR analysis

IR Spirit-Shimadzu was used to analyze the group content in the final nanocellulose product. Sample CNF was crushed and mixed well with KBr, then pressed into small pellets due to analysis. FTIR analysis was running in a wave range of 4000-400 cm^{-1}.

Oxidation Rate

Reaction rate coefficient was derived from Eqs. (2) and (3).

$$-\frac{dC}{dt} = k([OH^-] - [COOH]) \quad (2)$$

$$\ln([OH^-{}_0] - [COOH]_t) = -kt + ln[OH^-{}_0] \quad (3)$$

where $[OH^-{}_0]$ is represents the initial concentration of hydroxyl functional groups on nanocellulose and $[COOH]_t$ represents the concentration of carboxyl functional groups at t, t is oxidation time, and k is reaction rate coefficient. The concentration of the hydroxy group was determined by calculating anhydroglucose (AGU) groups in nanocellulose. One gram of nanocellulose contains 6.17 mmol AGU. Due to the glucose molecule form, about 50% of the hydroxy group can be oxidized (3.085 mmol hydroxy groups/gram) (Fraschini *et al.*, 2017).

Conductometry curves are shown in Figure 1.

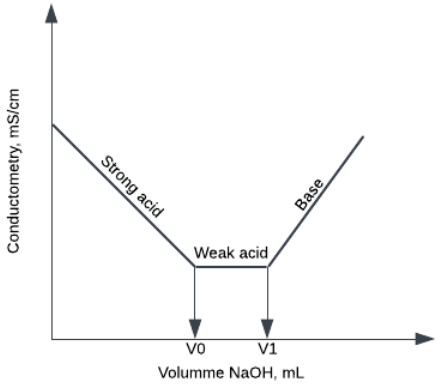

Fig. 1: Conductometry curves

Carboxylate groups calculated using Eq. (4) (Fraschini *et al.*, 2017).

$$[COOH] = \frac{(V_1 - V_0) \times C_{NaOH}}{m_{CNF}} \quad (4)$$

where V_0 and V_1 show the volume of NaOH shown in Figure 1, C_{NaOH} represents the concentration of NaOH (0.01 M), and m_{CNF} indicates the mass of CNF (0.2 gram).

RESULTS AND DISCUSSION

Nanocellulose was successfully produced from oil palm empty fruit bunch (OPEFB) through chemical treatment (delignification, bleaching, and acid hydrolysis). During the delignification process, using NaOH solution, the color changed from deep brown to bright yellow. This color indicates the disintegration of the amorphous structure in OPEFB caused by the loss of lignin and hemicellulose, called the defibrillation process (Neenu *et al.*, 2022). Lignin is black, so when lignin is dissolved in NaOH solution, the OPEFB color gets lighter. After the delignification process, hydrogen peroxide (H_2O_2) is used as a bleaching agent

to dissolve lignin and hemicellulose that remains in OPEFB after delignification.

Table 1 shows the percentage of lignin, hemicellulose, and cellulose in every step of the chemical treatment process of OPEFB. The delignification process can remove lignin and hemicellulose more than the bleaching process. In delignified oil palm empty fruit bunch (D-OPEFB), lignin has decreased by 7.44% and hemicellulose by 3.67%. Meanwhile, in the bleached oil palm empty fruit bunch (B-OPEFB), lignin and hemicellulose decrease by 1.44% and 1.33%. Despite bleaching having a negligible influence on removing lignin and hemicellulose, Figure 2 shows that the size of cellulose fibril after the bleaching process is shorter than before bleaching. This phenomenon is caused by using hydrogen peroxide as a bleaching agent that can degrade cellulose fibrils (Vera-Loor *et al.*, 2023).

Table 1. Lignin, hemicellulose, and cellulose content

Sample	Lignin, %	Hemi-cellulose, %	Cellulose, %	Water, %	Ash, %
OPEFB	26.47	23.50	32.98	11.55	5.51
D-OPEFB	19.03	19.82	46.65	12.42	2.10
B-OPEFB	17.59	18.49	52.12	11.61	0.89
CNF	14.46	13.26	61.78	10.39	0.26

The cellulose resulting from the delignification and bleaching processes is subsequently hydrolyzed using a 40% sulfuric acid (H_2SO_4) solution. During the acid hydrolysis, any remaining lignocellulosic residues, hemicellulose, and impurities that are insoluble in the alkaline solution is removed along with the acid, resulting in increased cellulose content in the sample. The size of cellulose after undergoing hydrolysis with acid decreases. In Figure 2, it can be observed that the size of cellulose fibrils after hydrolysis is extremely small, giving cellulose the appearance of fine powder. In powdered form, the cellulose size is expected to reach the nanoscale. The final cellulose nanofibrils (CNF) product after hydrolysis acid has a content of lignin 14.16%, hemicellulose 13.26%, and cellulose 61.78%. Another experiment explained the percentage of nanocellulose by adding 54% H_2SO4, which was 62.1% (Soetaredjo *et al.*, 2022).

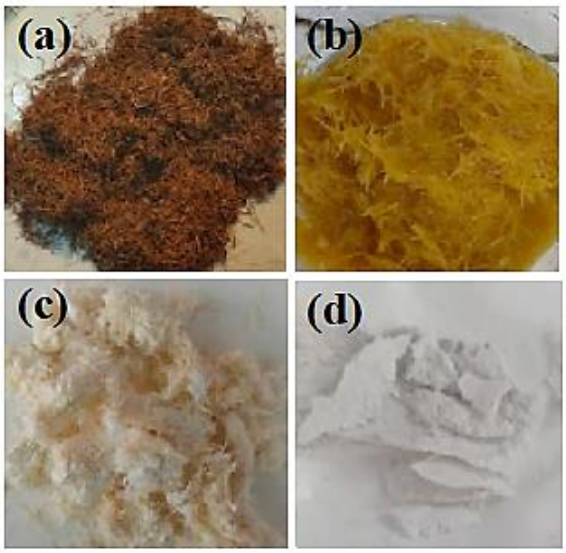

Fig. 2: (a) OPEFB (b) D-OPEFB (c) B-OPEFB (d) CNF.

Nanocellulose Size

To determine the precise dimension, nanocellulose was analyzed using PSA and TEM. The analysis using the PSA indicated a cellulose nanofibril (CNF) length of 127.4 nm. The nanocellulose diameter can be observed in Figure 3, which illustrates the analysis results using TEM. From the displayed images, it can be seen that the nanocellulose diameter is less than 10 nm.

By comparing the lengths of nanocellulose cross-sections, the specific diameter values of nanocellulose obtained are determined to be 4.80 nm, 6.24 nm, and 9.33 nm. In addition to the diameter ratio

calculations, Figure 3 compares the lengths of several nanocellulose specimens observed in the TEM analysis. Some nanocellulose fibers still exhibit 275 nm and 512 nm, indicating that nanocellulose lengths also vary.

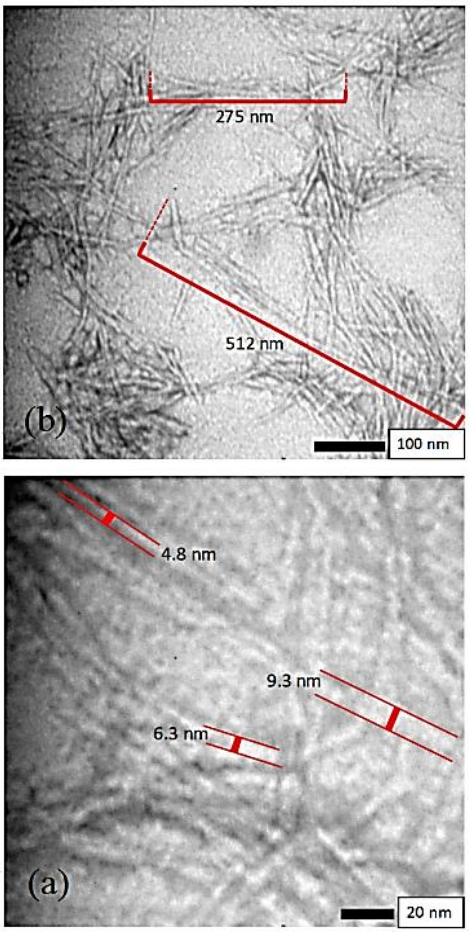

Fig. 3: (a) Comparison of nanocellulose diameter and (b) Comparison of nanocellulose length.

However, it can be observed that nanocellulose with a length of 127.4 nm is the predominant form. Therefore, it can be concluded that the nanocellulose produced in this study exhibits a size variation in the form of rod-like structures with lengths ranging from 127.4 nm to 512 nm and diameters less than 20 nm. The size of the nanocellulose in this experiment was smaller than that of others, which produced nanocellulose in the range of 579.8 nm to 640 nm. (Pranolo *et al.*, 2023). Rod-shaped nanocellulose is categorized as nanocellulose whiskers. Nanocellulose whiskers or cellulose nanofibers (CNF) are gained from natural fibers and characterized as rod-like shapes with lengths ranging from 10-1,000 nm and diameters of 5-20 nm (Zhou *et al.*, 2021). The results of this study align with the standard size specifications for nanocellulose whiskers.

Nanocellulose Crystallinity

During the chemical modification process to extract nanocellulose from OPEFB, several physical changes occurred in the sample, such as changes in color and size. Additionally, there were changes in the degree of crystallinity in the sample. From Figure 4, it can be observed that there are three peaks in the cellulose nanofibrils. These peaks are located at 15^0, 30^0, and 42.5^0. In the XRD analysis results of raw OPEFB, peaks only occur at 22^0. The peak intensities after chemical modification are higher, indicating that the chemical modification of OPEFB increases the crystallinity of nanocellulose. The degree of crystallinity of nanocellulose after the hydrolysis process is 58.1%. The crystallinity obtained from OPEFB nanocellulose in another experiment ranged from 34-55% (Hastuti *et al.*, 2019) and 51% (Ismail *et al.*, 2021).

The increase in crystallinity during the delignification, bleaching, and hydrolysis processes occurs due to the removal of amorphous structures. The crystalline structure of nanocellulose differs from the amorphous nature of lignin and hemicellulose. The molecules in the crystalline structure of nanocellulose are bound together by hydrogen bonds and Van der Waals forces, resulting in a solid and well-organized crystalline structure (Phanthong *et al.*, 2018). Hydronium ions break the

glycosidic bonds in the amorphous structure during hydrolysis, releasing crystallite structures, which increases the degree of crystallinity (Adawiyah *et al.*, 2022).

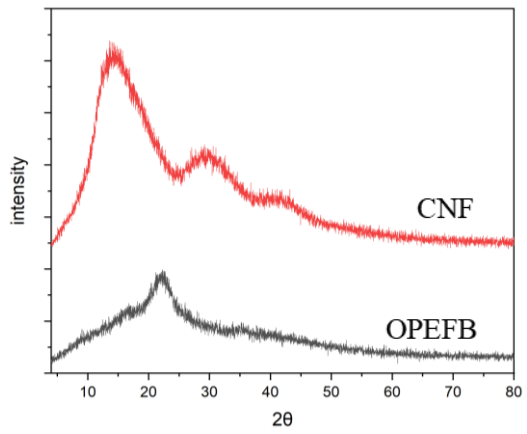

Fig. 4: XRD spectra from CNF and OPEFB.

The Effect of NaClO on the Total Acid Formed

A mechanism was established for calculating the carboxylate groups from oxidized nanocellulose by conductometric titration (Katz *et al.*, 1984). The nanocellulose carboxylate (1 g) was titrated using 0.1 M NaOH. Mol of natrium hydroxide consumed during titration was considered carboxylate groups (total acid) in the nanocellulose surface.

Figure 5 illustrates the total acid (carboxylate content) formation rate with varying additions of NaClO ranging from 4 mmol/gram to 20 mmol/gram. The addition of NaClO concentration influences the increase in total acid on the nanocellulose surface. The highest total acid content is achieved with NaClO 20 mmol/gram added, which amounts to 1,600 mmol/kg within a 16-minute reaction time. There is a nearly equal increase in acid groups for additions of NaClO in the range of 4 mmol/gram - 12 mmol/gram. However, at an addition of 16 mmol/gram of NaClO, there is a significant increase in total acid, rising from 690 mmol/kg to 1,292 mmol/kg. This increase is nearly double the total amount of adding 12 mmol/gram of NaClO.

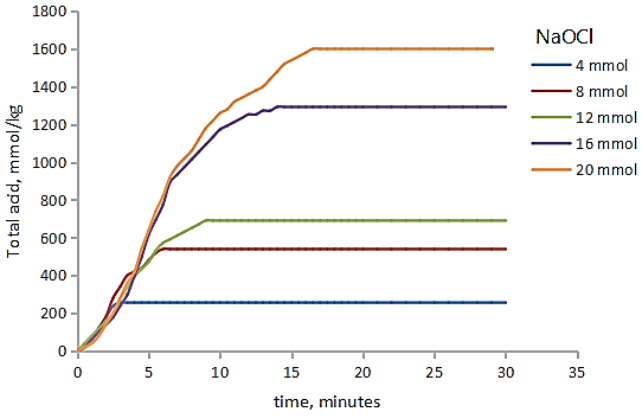

Fig. 5: The effect of NaClO variation on the total acid formed

Different concentrations of NaClO for the same reaction time will result in an equivalent amount of total acid if the oxidant is still applicable, as can be observed from the initial reaction rate curves, which overlap for all NaClO variations. In reactions with NaClO ratios of 8 mmol and 12 mmol/gram, the reactions overlap until both variations reach 532 mmol/kg at 5.5-minutes. Similarly, in reactions with NaClO ratios of 16 mmol/gram and 20 mmol/gram, the reactions overlap until they reach 620 mmol/kg at 6.5-minutes. After passing this point, the two curves no longer overlap, indicating that the availability of the oxidant in the smaller NaClO variations is nearing depletion. Therefore, the consumption rate of NaClO is assumed to be similar in all five cases. The similar total acid group formation rate at the same initial reaction time demonstrates the case. The higher reaction rate is only related to the greater oxidant availability from nanocellulose. Thus, the NaClO-related reaction rate shows zero-order kinetics and does not affect the reaction rate (Mao *et al.*, 2010).

In all cases, the reactions proceed rapidly and are completed within 20 minutes. Adding NaClO will increase the reaction time because more hydroxyl groups on nanocellulose can be oxidized. The reaction time is also related to the formation of steric hindrance, which blocks the oxidant from interacting with the hydroxyl groups. This steric hindrance appears from the aldehyde that reacts with hydroxyl groups to form a hemiacetal bond, which inhibits the oxidation reaction (Thi Thanh Hop *et al.*, 2022). Figure 4 shows that the reaction proceeds in two steps. The first step is the oxidation of primary alcohols on the surface of nanocellulose, which proceeds rapidly until the total acid reaches 256 mmol/kg. The first step is fast because there are still many accessible C_6 hydroxyl groups on the nanocellulose surface. The second step proceeds more slowly than the first step due to the decreasing accessibility of hydroxyl groups. As the reaction progresses, it slows down because unoxidized hydroxyl groups are located more profoundly and are less accessible. The condition of inaccessible hydroxyl groups can also lead to secondary reactions that produce chlorate and bromate (Saito *et al.*, 2010). The oxidation reaction decreases as the rate of acid group formation slows down until the oxidant is fully consumed (Sanchez-Salvador *et al.*, 2021).

The number of carboxylate groups formed determines the quality of nanocellulose adsorbent. Adsorption has been conducted with nanocellulose containing carboxylate groups of 260, 860, 1210, and 1500 mmol/kg with the ability to adsorb Cu metal of 0.5, 0.9, 1.4, and 1.75 mmol/g (Sehaqui *et al.*, 2014). Nanocellulose with 1400 mmol/kg carboxylate groups can adsorb Cu metal of 102.9 mg/g and Zn metal of 73.9 mg/g (Li *et al.*, 2019). By looking at the number of carboxylate groups formed in this study, which are 240, 532, 690, 1300, and 1600 mmol/kg, the nanocellulose adsorbent from OPEFB has met the requirements to adsorb metals.

Percent Recovery of Carboxylate Nanocellulose

Figure 6 illustrates the relationship between the addition of NaClO and mass recovery.

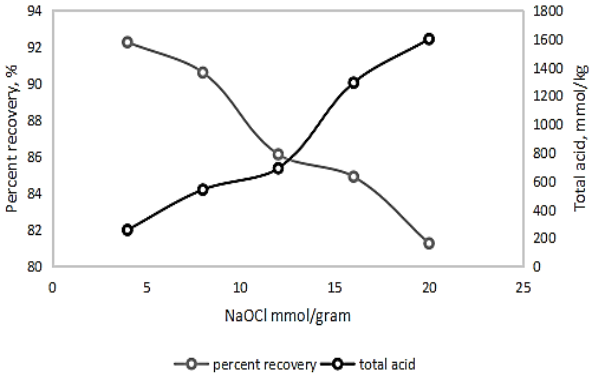

Fig. 6: Percent recovery of carboxylate nanocellulose in various NaClO

Within the range of NaClO additions from 4 mmol/gram to 8 mmol/gram, the mass recovery of nanocellulose remains above 90%. However, when NaClO is added at a ratio of 12 mmol/gram, there is a significant decrease in mass recovery, reaching 86%. The decrease in nanocellulose mass follows a linear equation with the addition of NaClO. This reduction in mass recovery is attributed to the degradation of the crystalline core of nanocellulose due to the penetration of NaClO (Fraschini *et al.*, 2017). The more NaClO is added, the greater the penetration into the crystalline core of nanocellulose, leading to observable degradation effects. Additionally, polymer chain cleavage of nanocellulose occurs because the oxidant attacks the 1,4-β-glycosidic bonds, resulting in smaller, amorphous chains that can readily dissolve in

the reaction medium (Saito *et al.*, 2005). Therefore, as more NaClO is added, the mass recovery in the sample decreases.

The Effect of NaClO on Functional Groups in Nanocellulose

Figure 7 illustrates the FTIR spectra for all samples exhibiting a broad peak in 3,500-3,300 cm^{-1}, indicating the stretching vibration of O-H groups in cellulose nanofibrils (CNF).

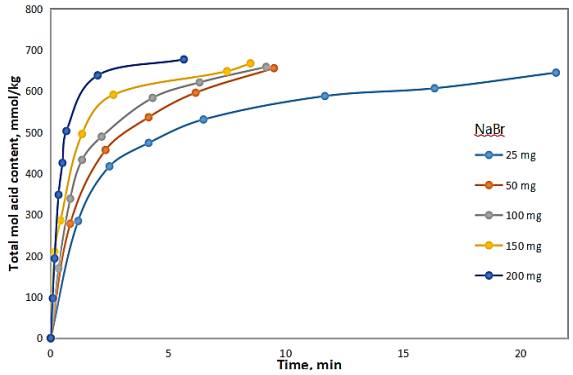

Fig. 7: FTIR spectra from CNF and CNF-oxidized

With the addition of NaClO, this region's intensity decreases due to oxidation of the secondary hydroxyl groups in nanocellulose (Coseri *et al.*, 2015). Stretching of C-H bonds also occurs at 2,900 cm^{-1}. In the nanocellulose spectrum, a peak at 1,640 cm^{-1} indicates the bending vibration of moisture associated with the O-H group (Thi Thanh Hop *et al.*, 2022). After oxidation, the peak at 1,640 cm^{-1} shifts toward 1,600 cm^{-1} with increasing NaClO. The carboxylate peak is detected at 1,615 cm^{-1} (Coseri *et al.*, 2015) and 1,600 cm^{-1} (Thi Thanh Hop *et al.*, 2022), corresponding to the formation of carboxylate groups (-COONa). In Figure 6, the peak at 1,640 cm^{-1} decreases, indicating a reduction in moisture bonding on nanocellulose. With the addition of NaClO, this peak shifts to 1,610 cm^{-1}, indicating the formation of carboxylate groups on the nanocellulose surface.

Unoxidized nanocellulose exhibits characteristic peaks, including a peak at 1,113 cm^{-1}, indicating stretching vibration of C-H deformation and asymmetric stretching at 1,163 cm^{-1} for C-H bonds. Additionally, there is a stretching vibration of C-O-C in the pyranose ring framework at 1,058 cm^{-1}. These characteristics tend to weaken with increasing oxidizer (Kim and Choi, 2014; Nikolic *et al.*, 2010). In all samples, there is evidence of decomposition during oxidation.

The Effect of NaBr on the Reaction Time

Figure 8 shows that with the addition of NaBr ranging from 50 mg to 200 mg, the reaction time is complete in less than 10 minutes. However, with the addition of 25 mg, the reaction time doubles. The addition of NaBr tends to accelerate the oxidation reaction of nanocellulose. However, with additions of 50 mg, 100 mg, and 150 mg, there is no significant increase in reaction time. This phenomenon occurs because the faster the carboxyl group forms, the faster the steric hindrance is formed (Thi Thanh Hop *et al.*, 2022). Steric hindrance will restrict the meeting of TEMPO radical ions with hydroxyl groups on the nanocellulose surface. Even though NaBr addition is doubled from the initial condition, the reaction time does not change much. The total acid formed in all NaBr variations is almost the same amount, ranging from 644-676 mmol/kg. Adding NaBr is unrelated to the amount of carboxyl groups formed on the nanocellulose surface.

Eq. 3 can be used to determine the constant of the nanocellulose oxidation reaction. Here, $[OH^-{}_0]$ represents the initial concentration of hydroxyl functional groups on nanocellulose at 3.085 mmol/kg [Fraschini, 2017], and $\ln([OH^-{}_0] - [COOH]_t)$ represents the difference in the initial concentration of hydroxyl groups and

carboxyl functional groups formed each time. Plotting $\ln([OH^-{}_0] - [COOH]_t)$ against time to obtain the reaction rate coefficient values for each NaBr addition can be seen in Figure 9.

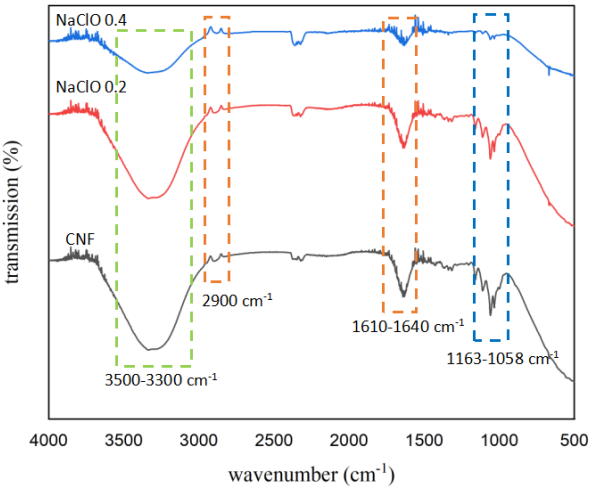

Fig. 8: The effect of NaBr variation on the reaction time

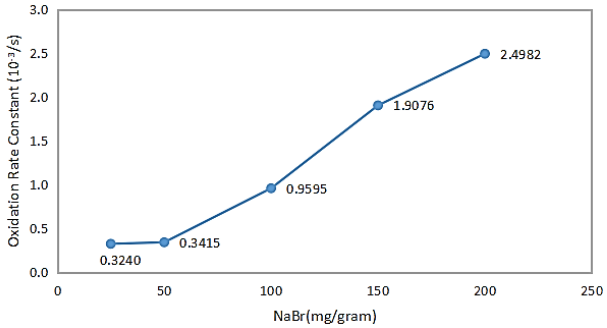

Fig. 9: The effect of NaBr variation on the reaction rate coefficient

Figure 8 shows that the constant reaction rate increases when 50 mg/gram is added to 200 mg/gram NaBr. The reaction rate is mostly the same with adding 25 mg/gram to 50 mg/gram NaBr. Further investigation is needed in the range of 50 mg/gram to 100 mg/gram to determine at what value of NaBr addition the reaction rate constant starts to increase.

CONCLUSION

Nanocellulose has been successfully obtained from the hydrolysis of OPEFB, with a length varying from 127.4 nm to 512 nm and a diameter below 20 nm. XRD results indicate that the crystallinity of nanocellulose increases after the acid hydrolysis process, reaching a value of 58.1% and cellulose content of 61.8%. In the oxidation reaction of nanocellulose in a TEMPO-mediated medium, the maximum total acid production is achieved by adding 20 mmol/gram of NaClO. This results in a total acid content of 1,600 mmol/kg in a 16-minute reaction time. As NaClO is added, there is a decrease in sample mass, indicating sample degradation. FTIR results demonstrate the decomposition of groups in nanocellulose during the oxidation process. All the reaction processes happened below 25 minutes, increasing the reaction rate by adding more than 50 mg/gram. Adding NaClO 12 mmol/gram and NaBr above 50 mg/gram produced a carboxylate group of 690 mmol/kg with a reaction time below 10 minutes. If NaBr is below 50 mg/gram, then at 10 minutes, the carboxylate group formed is below 690 mmol/kg when 12 NaClO mmol/gram is added.

ACKNOWLEDGEMENT

The authors acknowledge the financial support from the PMDSU scholarship, the Ministry of Research, Technology, and Higher Education, and the support from the Department of Chemical Engineering at Gadjah Mada University for the research facilities.

REFERENCES

Adawiyah, R., Suryanti, V., and Pranoto, 2022. "Preparation and characterization of microcrystalline cellulose from lembang (*Typha angustifolia L.*)." *J. Phys. Conf. Ser., 2190*.

Badan Pengelola Dana Perkebunan Kelapa Sawit, 2023. Grant Riset Sawit.

Bagheri, S., and Julkapli, N.M., 2018. "Chapter 12 - Grafted Nanocellulose as an Advanced Smart Biopolymer," in: Thakur, V.K.B.T.-B.G. (Ed.),. Elsevier, pp. 521–549.

Coseri, S., Biliuta, G., Zemljič, L.F., Srndovic, J.S., Larsson, P.T., Strnad, S., Kreže, T., Naderi, A., and Lindström, T., 2015. "One-shot carboxylation of microcrystalline cellulose in the presence of nitroxyl radicals and sodium periodate." *RSC Adv. 5*, 85889–85897.

de Nooy, A.E.J., Besemer, A.C., and van Bekkum, H., 1995. "Highly selective nitroxyl radical-mediated oxidation of primary alcohol groups in water-soluble glucans." *Carbohydr. Res. 269*, 89–98.

de Nooy, A.E.J., Besemer, A.C., and van Bekkum, H., 1994. "Highly selective tempo mediated oxidation of primary alcohol groups in polysaccharides." *Recl. des Trav. Chim. des Pays - Bas. 113*, 165–166.

Dewanti, D.P., 2018. "Potensi selulosa dari limbah tandan kosong kelapa sawit untuk bahan baku bioplastik ramah lingkungan." *J. Teknol. Lingkung. 19*, 81-87.

Eyley, S., and Thielemans, W., 2014. "Surface modification of cellulose nanocrystals." *Nanoscale 6*, 7764–7779.

Fraschini, C., Chauve, G., and Bouchard, J., 2017. "TEMPO-mediated surface oxidation of cellulose nanocrystals (CNCs)." *Cellulose 24*, 2775–2790.

Goldstein, S., and Samuni, A., 2007. "Kinetics and Mechanism of Peroxyl Radical Reactions with Nitroxides." *J. Phys. Chem. A. 111*, 1066–1072.

Habibi, Y., Chanzy, H., and Vignon, M.R., 2006. "TEMPO-mediated surface oxidation of cellulose whiskers." *Cellulose 13*, 679–687.

Hastuti, N., Kanomata, K., and Kitaoka, T., 2019. "Characteristics of TEMPO-oxidized cellulose nanofibers from oil palm empty fruit bunches produced by different amounts of oxidant." *IOP Conf. Ser. Earth Environ. Sci. 359*, 012008.

Hastuti, N., Setiawan, H., Kanomata, K., and Kitaoka, T., 2022. "Cellulose nanofibers of oil palm biomass in alginate-based membranes for water-ethanol mixture separation." *Cellul. Chem. Technol. 56*, 737–747.

Hidayatulloh, I., Widyanti, E. M., Aztaris, C., Melanitria, A., and Elizabeth, L., 2022. "Kajian pustaka sintesis nanoselulosa dari tandan kosong kelapa sawit sebagai filler pembuatan tisu toilet." *FLUIDA 15 (1)*, 51–59.

Hidayatulloh, I., Widyanti, E.M., Kusumawati, E., and Elizabeth, L., 2021. "Nanocellulose production from empty palm oil fruit bunches (EPOFB) using hydrolysis followed by freeze drying." *ASEAN J. Chem. Eng., 21*, 52–61.

Husin, A. and Hasibuan, A. 2020. "Studi pengaruh variasi konsentrasi asam posfat (H_3PO_4) dan waktu perendaman karbon terhadap karakteristik karbon aktif dari kulit durian." *J. Tek. Kim., USU 9 (2)*, 80–86.

Indarti, E., Marwan, and Wanrosli, W.D., 2015. "Thermal stability of oil palm empty fruit bunch (OPEFB) nanocrystalline cellulose: Effects of post-treatment of oven drying and solvent exchange techniques." *J.*

Phys. Conf. Ser. 622, 012025.

Ismail, F., Othman, N.E.A., Wahab, N.A., Hamid, F.A., and Aziz, A.A., 2021. "Preparation of microcrystalline cellulose from oil palm empty fruit bunch fibre using steam-assisted acid hydrolysis." *J. Adv. Res. Fluid Mech. Therm. Sci. 81*, 88–98.

Isogai, A., Saito, T., and Fukuzumi, H., 2011. "TEMPO-oxidized cellulose nanofibers." *Nanoscale 3*, 71–85.

Iwamoto, S., Isogai, A., and Iwata, T., 2011. "Structure and mechanical properties of wet-spun fibers made from natural cellulose nanofibers". *Biomacro-molecules 12 (3),* 831–836.

Katz, S., Beatson, R.P., and Anthony, M., 1984. "The determination of strong and weak acidic groups in sulfite pulps." *Sven. Papperstidning-nordisk Cellul. 87*, 48–53.

Kim, J., and Choi, H., 2014. "Cationization of periodate-oxidized cotton cellulose with choline chloride." *Cellul. Chem. Technol., 48*, 25–32.

Levanič, J., Šenk, V.P., Nadrah, P., Poljanšek, I., Oven, P., and Haapala, A., 2020. "Analyzing TEMPO-oxidized cellulose fiber morphology: New insights into optimization of the oxidation process and nanocellulose dispersion quality." *ACS Sustain. Chem. Eng. 8*, 17752–17762.

Li, M., Messele, S.A., Boluk, Y., and Gamal El-Din, M., 2019. "Isolated cellulose nanofibers for Cu (II) and Zn (II) removal: performance and mechanisms." *Carbohydr. Polym. 221*, 231–241.

Liu, P., Garrido, B., Oksman, K., and Mathew, A.P., 2016. "Adsorption isotherms and mechanisms of Cu(II) sorption onto TEMPO-mediated oxidized cellulose nanofibers." *RSC Adv. 6*, 107759–107767.

Mao, L., Ma, P., Law, K., Daneault, C., and Brouillette, F., 2010. "Studies on kinetics and reuse of spent liquor in the TEMPO-mediated selective oxidation of mechanical pulp." *Ind. Eng. Chem. Res. 49*, 113–116.

Martínez-Ramírez, A.P., Rincón-Ortiz, S.A., and Blanco-Tirado, C., 2023. "TEMPO oxidation for high cellulose content biomass: A study on palm oil empty fruit bunch fibers". *Res. Square*, 1–25. DOI: 10.21203/rs.3.rs-3186311/v1

Neenu, K. V., Midhun Dominic, C.D., Begum, P.M.S., Parameswaranpillai, J., Kanoth, B.P., David, D.A., Sajadi, S.M., Dhanyasree, P., Ajithkumar, T.G., and Badawi, M., 2022. "Effect of oxalic acid and sulphuric acid hydrolysis on the preparation and properties of pineapple pomace derived cellulose nanofibers and nanopapers." *Int. J. Biol. Macromol. 209*, 1745–1759.

Nikolic, T., Kostic, M., Praskalo, J., Pejic, B., Petronijevic, Z., and Skundric, P., 2010. "Sodium periodate oxidized cotton yarn as carrier for immobilization of trypsin." *Carbohydr. Polym. 82*, 976–981.

Phanthong, P., Reubroycharoen, P., Hao, X., Xu, G., Abudula, A., and Guan, G., 2018. "Nanocellulose: Extraction and application." *Carbon Resour. Convers. 1*, 32–43.

Pranolo, S.H., Waluyo, J., Ikbar, R., Damayanthy, R.A., Lestary, S., and Qadarusman, M.L., 2023. "Application of nanocrystal cellulose based on empty palm oil fruit bunch as glucose biosensing." *ASEAN J. Chem. Eng. 23*, 360–369.

Saito, T., Hirota, M., Tamura, N., and Isogai, A., 2010. "Oxidation of bleached wood pulp by TEMPO/NaClO/$NaClO_2$ system: effect of the oxidation conditions on carboxylate content and degree of polymerization." *J. Wood Sci. 56*, 227–232.

Saito, T., Yanagisawa, M., and Isogai, A., 2005. "TEMPO-mediated oxidation of native cellulose: SEC–MALLS analysis of water-soluble and insoluble fractions in the oxidized products." *Cellulose 12*, 305–315.

Sanchez-Salvador, J., Campano, C., Negro, C., Monte, M., and Blanco, A., 2021. "Increasing the possibilities of TEMPO - mediated oxidation in the production of cellulose nanofibers by reducing the reaction time and reusing the reaction medium." *Adv. Sustain. Syst. 5*. 2000277.

Segal, L., Creely, J.J., Martin, A.E., and Conrad, C.M., 1959. "An empirical method for estimating the degree of crystallinity of native cellulose using the X-ray diffractometer." *Text. Res. J. 29*, 786–794.

Sehaqui, H., de Larraya, U.P., Liu, P., Pfenninger, N., Mathew, A.P., Zimmermann, T., and Tingaut, P., 2014. "Enhancing adsorption of heavy metal ions onto biobased nanofibers from waste pulp residues for application in wastewater treatment." *Cellulose 21*, 2831–2844.

Singla, R., Abidi, S.M.S., Dar, A.I., and Acharya, A., 2019. "Nanomaterials as potential and versatile platform for next generation tissue engineering applications." *J. Biomed. Mater. Res. - Part B Appl. Biomater. 107*, 2433–2449.

Soetaredjo, F.E., Santoso, S.P., Waworuntu, G.L., and Darsono, F.L., 2022. "Cellulose nanocrystal (CNC) capsules from oil palm empty fruit bunches (OPEFB)." *Biointerface Res. Appl. Chem. 12*, 2013–2021.

Thi Thanh Hop, T., Thi Mai, D., Duc Cong, T., Thi Y. Nhi, T., Duc Loi, V., Thi Mai Huong, N., and Trinh Tung, N., 2022. "A comprehensive study on preparation of nanocellulose from bleached wood pulps by TEMPO-mediated oxidation." *Results Chem. 4*, 100540.

Thomas, B., Raj, M.C., B, A.K., H, R.M., Joy, J., Moores, A., Drisko, G.L., and Sanchez, C., 2018. "Nanocellulose, a versatile green platform: From biosources to materials and their applications." *Chem. Rev. 118*, 11575–11625.

Vera-Loor, A., Rigou, P., Mortha, G., and Marlin, N., 2023. "Oxidation treatments using hydrogen peroxide to convert paper-grade eucalyptus kraft pulp into dissolving-grade pulp." *Molecules 28*, 7927.

Xhanari, K., Syverud, K., Chinga-Carrasco, G., Paso, K., and Stenius, P., 2011. "Reduction of water wettability of nanofibrillated cellulose by adsorption of cationic surfactants." *Cellulose 18*, 257–270.

Xu, S., Huo, D., Wang, K., Yang, Q., Hou, Q., and Zhang, F., 2021. "Facile preparation of cellulose nanofibrils (CNFs) with a high yield and excellent dispersibility via succinic acid hydrolysis and $NaClO_2$ oxidation." *Carbohydr. Polym. 266*, 118118.

Yiin, C.L., Ho, S., Yusup, S., Quitain, A.T., Chan, Y.H., Loy, A.C.M., and Gwee, Y.L., 2019. "Recovery of cellulose fibers from oil palm empty fruit bunch for pulp and paper using green delignification approach." *Bioresour. Technol. 290*, 121797.

Zhou, Z., Li, Y., and Zhou, W., 2021. "The progress of nanocellulose in types and preparation methods." *J. Phys. Conf. Ser. 1, 012042*.

Zinge, C., and Kandasubramanian, B., 2020. "Nanocellulose based biodegradable polymers." *Eur. Polym. J. 133*, 109758.